



## True to Milankovitch: Glacial Inception in the New Community Climate System Model

MARKUS JOCHUM, ALEXANDRA JAHN, SYNTE PEACOCK, DAVID A. BAILEY,  
JOHN T. FASULLO, JENNIFER KAY, SAMUEL LEVIS, AND BETTE OTTO-BLIESNER

*National Center for Atmospheric Research, Boulder, Colorado*

(Manuscript received 19 January 2011, in final form 25 August 2011)

### ABSTRACT

The equilibrium solution of a fully coupled general circulation model with present-day orbital forcing is compared to the solution of the same model with the orbital forcing from 115 000 years ago. The difference in snow accumulation between these two simulations has a pattern and a magnitude comparable to the ones inferred from reconstructions for the last glacial inception. This is a major improvement over previous similar studies, and the increased realism is attributed to the higher spatial resolution in the atmospheric model, which allows for a more accurate representation of the orography of northern Canada and Siberia. The analysis of the atmospheric heat budget reveals that, as postulated by Milankovitch's hypothesis, the only necessary positive feedback is the snow–albedo feedback, which is initiated by reduced melting of snow and sea ice in the summer. However, this positive feedback is almost fully compensated by an increased meridional heat transport in the atmosphere and a reduced concentration of low Arctic clouds. In contrast to similar previous studies, the ocean heat transport remains largely unchanged. This stability of the northern North Atlantic circulation is explained by the regulating effect of the freshwater import through the Nares Strait and Northwest Passage and the spiciness import by the North Atlantic Current.

### 1. Introduction

Over the last 400 000 years the earth's climate went through several glacial and interglacial cycles, which are correlated with changes in its orbit and associated changes in insolation (Milankovitch 1941; Hays et al. 1976; Huybers and Wunsch 2004). Over this time, changes in global ice volume, temperature, and atmospheric  $\text{CO}_2$  have been strongly correlated with each other (Petit et al. 1999; Rohling et al. 2009). The connection between temperature and ice volume is not surprising, and a strong snow/ice–albedo feedback makes it plausible to connect both to changes in the earth's orbit [see, however, Tziperman et al. (2006) for a discussion of alternative hypotheses].

Models of intermediate complexity (e.g., Sytkus et al. 1994; Crucifix and Loutre 2001; Khodri et al. 2001; Wang and Mysak 2002; Khodri et al. 2003; Kageyama et al. 2004; Calov et al. 2005; Ganopolski et al. 2010) and flux-corrected GCMs (Groeger et al. 2007; Kaspar and

Cubasch 2007) have typically been able to simulate a connection between orbital forcing, temperature, and snow volume. So far, however, fully coupled, nonflux-corrected primitive equation general circulation models (GCMs) have failed to reproduce glacial inception, the cooling and increase in snow and ice cover that leads from the warm interglacials to the cold glacial periods (e.g., Vettoretti and Peltier 2003; Born et al. 2010; Jochum et al. 2010, hereafter JPML). Milankovitch (1941) postulated that the driver for this cooling is the orbitally induced reduction in Northern Hemisphere summertime insolation and the subsequent increase of perennial snow cover. The increased perennial snow cover and its positive albedo feedback are, of course, only precursors to ice sheet growth. The GCMs failure to recreate glacial inception [see Otieno and Bromwich (2009) for a summary], which indicates a failure of either the GCMs or of Milankovitch's hypothesis. Of course, if the hypothesis would be the culprit, one would have to wonder if climate is sufficiently understood to assemble a GCM in the first place. Either way, it appears that reproducing the observed glacial–interglacial changes in ice volume and temperature represents a good test bed for evaluating the fidelity of some key model feedbacks relevant to climate projections.

*Corresponding author address:* Markus Jochum, National Center for Atmospheric Research, P.O. Box 3000, Boulder, CO 80307.  
E-mail: markus@ucar.edu

The potential causes for GCMs failing to reproduce inception are plentiful, ranging from numerics (Vettoretti and Peltier 2003) on the GCMs side to neglected feedbacks of land, atmosphere, or ocean processes (e.g., Gallimore and Kutzbach 1996; Hall et al. 2005; JPML; respectively) on the theory side. It is encouraging, though, that for some GCMs it takes only small modifications to produce an increase in perennial snow cover (e.g., Dong and Valdes 1995). Nevertheless, the goal for the GCM community has to be the recreation of increased perennial snow cover with a GCM that has been tuned to the present-day climate, and is subjected to changes in orbital forcing only.

The present study is motivated by the hope that the new class of GCMs that has been developed over the last 5 years [driven to some extent by the forthcoming Fifth Assessment Report (AR5)], and incorporates the best of the climate community's ideas, will finally allow us to reconcile theory and GCM results. It turns out that at least one of the new GCMs is true to the Milankovitch hypothesis. The next section will describe this GCM and illustrate the impact of changing present-day insolation to the insolation of 115 000 years ago (115 kya). Section 3 then analyzes in detail the Arctic heat budget with its multitude of positive and negative feedbacks, and section 4 analyzes the reorganization of the Atlantic meridional overturning circulation (AMOC). Section 5 concludes the study with a summary and implications for future model development. The two main goals of the present work are to demonstrate that the 115-kya orbital changes produce a realistic increase in snow cover in the Community Climate System Model, version 4 (CCSM4), and to quantify the relevant climate feedbacks.

## 2. Model description

The numerical experiments are performed using the latest version of the National Center for Atmospheric Research (NCAR) CCSM4, which consists of the fully coupled atmosphere, ocean, land, and sea ice models. A description of this version can be found in Gent et al. (2011). The ocean component has a horizontal resolution that is constant at  $1.125^\circ$  in longitude and varies from  $0.27^\circ$  at the equator to approximately  $0.7^\circ$  in the high latitudes. In the vertical there are 60 depth levels; the uppermost layer has a thickness of 10 m and the deepest layer has a thickness of 250 m. The atmospheric component uses a horizontal resolution of  $0.9^\circ \times 1.25^\circ$  with 26 levels in the vertical. The sea ice model shares the same horizontal grid as the ocean model and the land model is on the same horizontal grid as the atmospheric model. The details of the different model components are described in the papers of this special issue;

for the present purpose, it is sufficient to know that CCSM4 is a state-of-the-art climate model that has improved in many aspects from its predecessor CCSM3 (Gent et al. 2011). For the present context, the most important improvement is the increased atmospheric resolution, because it allows for a more accurate representation of altitude and therefore land snow cover (see the next section).

The subsequent sections will analyze and compare two different simulations: an 1850 control (CONT), in which the earth's orbital parameters are set to the 1990 values and the atmospheric composition is fixed at its 1850 values [for details of the atmospheric composition see Gent et al. (2011)]; and a simulation identical to CONT, with the exception of the orbital parameters, which are set to the values of 115 kya (OP115). The atmospheric  $\text{CO}_2$  concentration in both experiments is 285 ppm. CONT was integrated for 700 years, and OP115 was branched off from CONT after year 500 and continued for 300 years. Unless otherwise noted, the comparisons will be done between the means of years 651–700 of CONT and the years 751–800 of OP115. Although CONT is considered fully spun up the comparison is not quite clean, because there is a small drift in ocean temperature and salinity. The two different time intervals were chosen because at year 700 the AMOC in OP115 did not reach equilibrium yet, and we did not have the computational resources to extend CONT beyond year 700. However, in the present context the drift is negligible because it is mostly confined to the abyssal ocean (Danabasoglu et al. 2012).

This experimental setup is not optimal, of course. Ideally one would like to integrate the model from the last interglacial, approximately 126 kya ago (e.g., Waelbroeck et al. 2002; Thompson and Goldstein 2005), for 10 000 years into the glacial with slowly changing orbital forcing. However, this is not affordable; a 100-yr integration of CCSM on the NCAR supercomputers takes approximately 1 month and a substantial fraction of the climate group's computing allocation. Instead, we assume that the atmosphere, land, and upper ocean have forgotten their initial conditions after 200 years (see Collins et al. 2006), and that the climate system over the last 130,000 years did not have multiple equilibria. The latter cannot be proven, but the authors are not aware of a single study that indicates multiple equilibria in full GCMs [see, however, Stommel (1961) for a classic study of multiple equilibria in idealized systems]. Even if one is forced to accept the current time-slice comparison as inevitable but reasonable, it would be preferable to use the last rather than the present interglacial as the control, in particular for the analysis of the transient ocean response. Again, costs are a problem. More importantly

though, it is the main result of the ocean transient study that the meridional ocean heat transport is quite stable, even in the face of large perturbations, and that ocean mechanisms are not necessary to explain glacial inception (at least not in the present model). Thus, we claim that the details of the interglacials are secondary for the current study, and do not justify the substantially larger costs arising from the attempt to reproduce the details of the last interglacials.

The CCSM does not yet contain an ice sheet module, so we use snow accumulation as the main metric to evaluate the inception scenario. The snow accumulation on land is computed as the sum of snowfall, frozen rain, snowmelt, and removal of excess snow. Excess snow is defined as snow exceeding 1 m of water equivalent, approximately 3–5 m of snow. This excess snow removal is a very crude parameterization of iceberg calving, and together with the meltwater the excess snow is delivered to the river network, and eventually added to the coastal surface waters of the adjacent ocean grid cells (for more details see Oleson et al. 2010; Lawrence et al. 2010). Thus, the local ice sheet volume and the global freshwater volume are conserved. For the Greenland ice sheet in CONT the annual mean freshwater discharge is  $1100 \text{ km}^3 \text{ yr}^{-1}$ , and for the Antarctic ice sheet it is  $2400 \text{ km}^3 \text{ yr}^{-1}$ ; the latter compares well with the observational estimates of  $2300 \text{ km}^3 \text{ yr}^{-1}$  (Vaughan et al. 1999). The Greenland freshwater discharge, however, is almost twice the observed value of  $600 \text{ km}^3 \text{ yr}^{-1}$  (Reeh et al. 1999), a reflection of the Greenland precipitation biases in CCSM4 (Gent et al. 2011).

Another bias relevant for the present discussion is the temperature bias of the northern high-latitude land. As discussed in the next section, much of the CCSM4 response to orbital forcing is due to reduced summer melt of snow. A cold bias in the control will make it more likely to keep the summer temperature below freezing, and will overestimate the model's snow accumulation. In the annual mean, northern Siberia and northern Canada are too cold by about  $1^\circ\text{C}$ – $2^\circ\text{C}$ , and Baffin Island by about  $5^\circ\text{C}$  (Gent et al. 2011). The Siberian biases are not so dramatic, but it is quite unfortunate that Baffin Island, the nucleus of the Laurentide ice sheet, has one of the worst temperature biases in CCSM4. A closer look at the temperature biases in North America, though, reveals that the cold bias is dominated by the fall and winter biases, whereas during spring and summer Baffin Island is too cold by approximately  $3^\circ\text{C}$ , and the Canadian Archipelago even shows a weak warm bias (Peacock 2012).

The particular time period for the orbital forcing of OP115 is chosen because the solar forcing at  $65^\circ\text{N}$  during June differs from its present value by approximately

$34 \text{ W m}^{-2}$  or 7%, more than during most other epochs (Berger and Loutre 1991). Moreover, observations suggest that the onset of the last ice age dates around this time (Andrews and Mahaffy 1976; Petit et al. 1999; Thompson and Goldstein 2005; Capron et al. 2010). The change in orbital parameters means that particularly at northern high latitudes there is less insolation during spring and early summer months, and more radiation later in the fall. This shift in the seasonal distribution of insolation is at the heart of the orbit-based inception hypothesis, because it leads to increased snow and sea ice cover during early summer, and a positive snow/ice–albedo feedback (Milankovitch 1941, section 123). Note that a changing orbit leads to differently defined seasons (e.g., Timm et al. 2008), but this does not affect the present analysis. If annual minima or maxima are discussed (like for the insolation above), they are always based on an average over the same month from both integrations, and they also always occur in the same month in both integrations.

### 3. Land and atmosphere response

In the annual mean the differences in orbital parameters between OP115 and CONT lead to a warmer tropical band, and cooler northern high latitudes (Fig. 1a), with maximum cooling in July of  $11^\circ\text{C}$  in northern Siberia and  $8^\circ\text{C}$  in the Canadian Archipelago (not shown). There is only little response in the southern high latitudes, and that is mostly confined to the ocean. To isolate the impact of the ocean on glacial–interglacial dynamics, we replaced the full ocean model with a slab-ocean model. The slab-ocean model prescribes the monthly mean distribution of mixed layer depth and heat transport from CONT, and comes to equilibrium after 20 years (Danabasoglu and Gent 2009). Thus, the ocean heat transport in the slab-ocean configuration of CONT and OP115 are identical, but the SST and climate can be different. The two respective setups are integrated for 60 years, and the temperature differences between OP115 and CONT in this configuration are quite similar (Fig. 1b; snow and sea ice differences are similar too, but not shown), with the full ocean leading to a slightly weaker response. The exception is the Labrador Sea, which shows approximately  $2^\circ\text{C}$  more cooling with a full ocean model. While Southern Hemisphere and tropical temperature differences between both sets of experiments are similar to the coarse-resolution results of JPML, the northern high-latitude response is significantly weaker. This can be attributed to the different response of the AMOC, and will be the focus of the next section.

The colder northern high latitudes in OP115 are associated with significant increase in snow accumulation

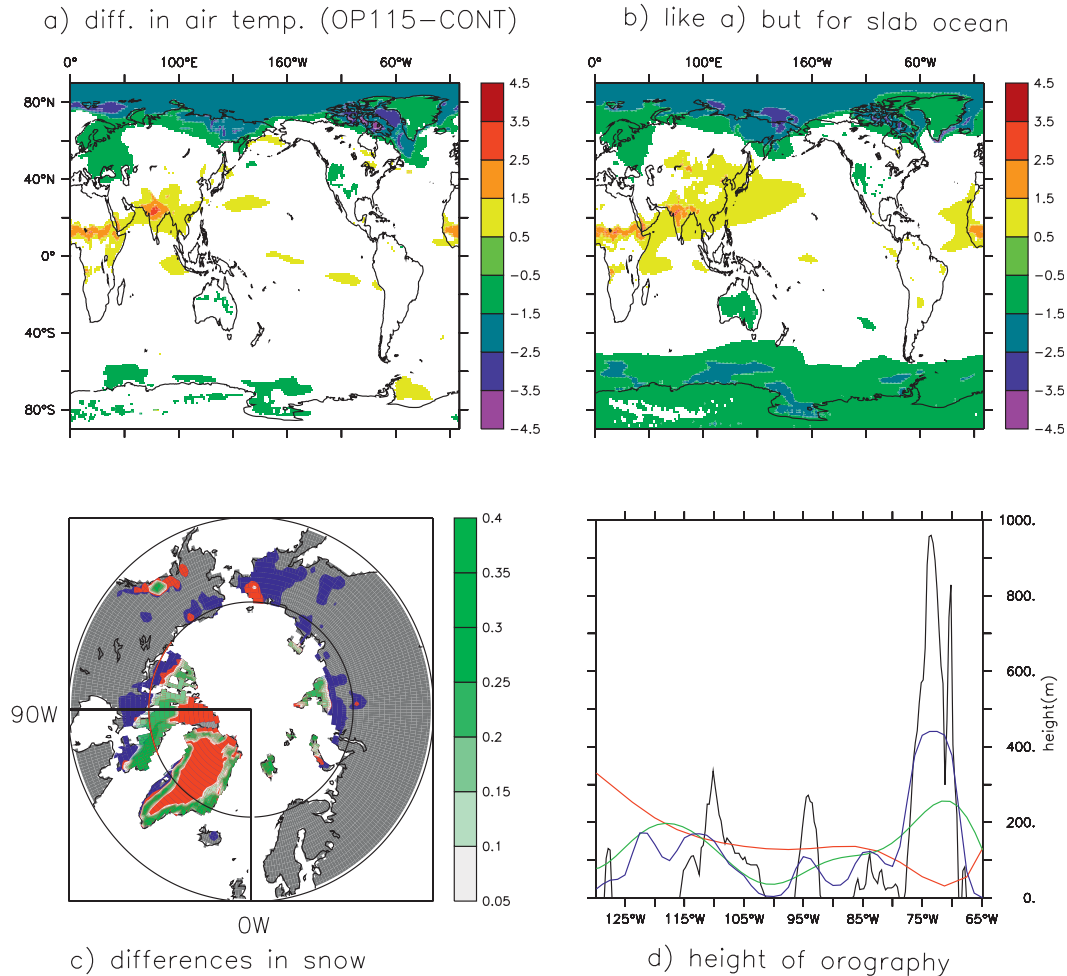


FIG. 1. (a) Difference in annual mean surface temperature between OP115 and CONT and (b) between their respective slab-ocean counterparts. (c) Area where the summer (minimum) snow depth is larger than 1 cm for CONT (red), and its increase in OP115 (blue). The overlaid green shades quantify the difference in annual mean snow accumulation ( $\text{m yr}^{-1}$ ). (d) Orography height along the  $70^\circ\text{N}$  parallel from Baffin Island to Banks Island [red line in (c)]. Black: Observed (ETOPO20; Edwards 1986). Red: T31 spectral core ( $\approx 4^\circ$  resolution). Green: T85 spectral core ( $\approx 2^\circ$  resolution). Blue:  $1^\circ$  finite-volume core.

in Greenland, the Canadian Archipelago, and northern Siberia (Fig. 1c), the latter two being the origination points for the glacial ice sheets in ice sheet reconstructions (Svendsen et al. 2004; Kleman et al. 2010). The isolated inland points of increased accumulation are associated with Mount McKinley, the high point of the Rocky Mountains (6000 m, CCSM: 1500 m), and the high point of the Chukotskiy Range in Siberia [1900 m, CCSM: 500 m; note, though, that the glacial history of East Siberia is under debate; Gualtieri et al. (2003)]. The increase in snow depth is almost solely due to reduced summer melt (not shown). This cooling and reduced melt is also reflected in the freshwater discharge of Greenland, where the total discharge (parameterized calving plus meltwater runoff) is reduced by 10% to

$1000 \text{ km}^3 \text{ yr}^{-1}$ , but the meltwater discharge is reduced by 40%, from 570 to  $310 \text{ km}^3 \text{ yr}^{-1}$ . On the other hand, the Antarctic freshwater discharge (and precipitation, of course) between the two experiments is identical to within 2%.

Apart from modifications to the deep convection parameterization (Neale et al. 2008), the atmosphere physics of CCSM4 is identical to its predecessor's, CCSM3, which did not produce realistic snow accumulation patterns in inception scenarios (JPML; Vettoretti and Peltier 2011); the latter even reduced the greenhouse gas concentrations by 10%. This suggests that horizontal resolution plays a key role, which is confirmed when one analyzes the representation of orography in different resolutions (Fig. 1d): increased resolution allows for higher

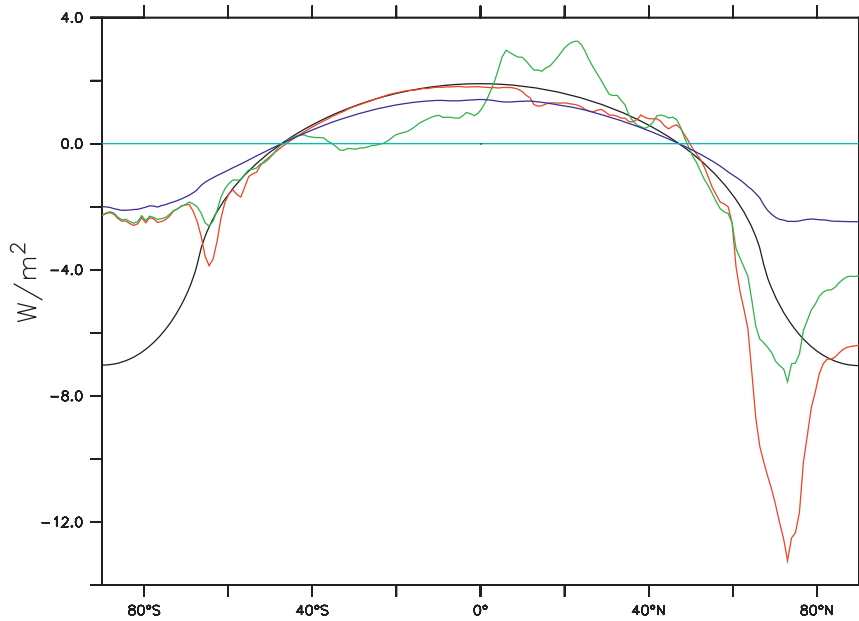


FIG. 2. Difference of zonally averaged flux at the TOA (OP115–CONT). Black: insolation. Blue: insolation times albedo of CONT. Red: clear-sky net shortwave radiation. Green: net shortwave radiation.

mountain peaks. When combined with the adiabatic lapse rate, this will lead to cooler summers and less melting (see also Vettoretti and Peltier 2003; Vavrus et al. 2011).

The pattern and amplitude of wind stress and precipitation response is similar to the one in the coarse-resolution study of JPML, involving minor changes with the exception of a stronger Indian summer monsoon and stronger westerlies over the North Pacific (not shown). In particular the zonally averaged wind stress over the Southern Ocean is identical to within 0.5%, and its maximum is at the same latitude. As illustrated in Fig. 1 the main differences between OP115 and CONT are in the Arctic and will be analyzed here.

The difference in orbital forcing between OP115 and CONT leads to larger incoming radiation at the top of the atmosphere (TOA) in the tropics and smaller radiation at high latitudes in the former compared to the latter (Fig. 2), with the total incoming solar radiation being  $0.3 \text{ W m}^{-2}$  larger in OP115 than in CONT. Our focus will be on the Northern Hemisphere north of  $60^\circ\text{N}$ , which covers the areas of large cooling and increased snow cover (Fig. 1). Compared to CONT, the annual average of the incoming radiation over this Arctic domain is smaller in OP115 by  $4.3 \text{ W m}^{-2}$  (black line), but the large albedo reduces this difference at the TOA to only  $1.9 \text{ W m}^{-2}$  (blue line, see also Table 1). This is only a minor change, and the core piece of the Milankovitch hypothesis is how this signal is spread across the seasonal cycle and amplified (e.g., Imbrie et al. 1992): reduced

summer insolation prolongs the time during which land is covered with snow, and ocean covered with ice. In CCSM4 this larger albedo in OP115 leads to a TOA clear-sky shortwave radiation that is  $8.6 \text{ W m}^{-2}$  smaller than in CONT (red line; clear-sky radiation is diagnosed during the simulation by omitting the clouds from the radiation calculation)—more than 4 times the original signal. The snow/ice–albedo feedback is then calculated as  $6.7 \text{ W m}^{-2}$  ( $8.6-1.9 \text{ W m}^{-2}$ ). Interestingly, the low cloud cover is smaller in OP115 than in CONT, reducing the difference in total TOA shortwave radiation by  $3.1$  to  $5.5 \text{ W m}^{-2}$  (green line). Summing up, an initial forcing of  $1.9 \text{ W m}^{-2}$  north of  $60^\circ\text{N}$ , is amplified through the snow–ice–albedo feedback by  $6.7 \text{ W m}^{-2}$ , and damped through a negative cloud feedback by  $3.1 \text{ W m}^{-2}$ .

The negative feedback of the clouds is mostly due to a reduction of low cloud cover over the ocean and coastal areas during summer, which leads to reduced reflectivity

TABLE 1. Summary of the annual mean heat flux feedbacks north of  $60^\circ\text{N}$ .

Process	Strength ( $\text{W m}^{-2}$ )
Insolation forcing	+4.3
× Present-day albedo	−2.4
Snow/ice–albedo feedback	+6.7
Low cloud–sea ice feedback	−3.1
Meridional heat transport feedback	−3.1
Total forcing	+2.4

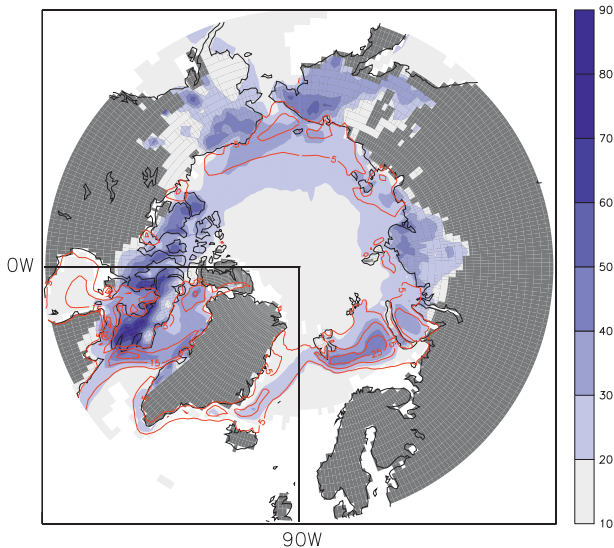


FIG. 3. Difference in maximum (July) shortwave cloud forcing (blue shades,  $\text{W m}^{-2}$ ) and minimum (July) sea ice concentration (contour interval 10%). Only forcing differences  $>10 \text{ W m}^{-2}$  are shown; in the coastal areas the blue shades of this signal may overlay the gray landmass. There are no areas of reduced forcing change  $<-10 \text{ W m}^{-2}$ .

or shortwave cloud forcing (Fig. 3). These high-latitude stratus clouds have a similar effect as snow or ice: they reflect sunlight. Unlike at lower latitudes, Arctic low cloud formation via coupling with the ocean is frequently inhibited by sea ice and surface temperature inversions. While the presence of open water in the Arctic does not guarantee atmosphere–ocean coupling and low cloud formation, open water has been shown to increase Arctic cloud cover when atmosphere–ocean coupling is strong (Kay and Gettelman 2009). Since the Arctic Ocean in OP115 is colder and has more sea ice cover than in CONT, especially in summer, reductions in low cloud amount are not surprising, and serve to counteract the positive ice–albedo feedback from increased sea ice cover.

Because of the larger meridional temperature (Fig. 1a) and moisture gradient (Fig. 4a), the lateral atmospheric heat flux into the Arctic is increased from 2.88 to 3.00 PW. This 0.12 PW difference translates into an Arctic average of  $3.1 \text{ W m}^{-2}$ ; this is a negative feedback as large as the cloud feedback, and 6 times as large as the increase in the ocean meridional heat transport at  $60^\circ\text{N}$  (next section). Thus, the negative feedback of the clouds and the meridional heat transport almost compensate for the positive albedo feedback, leading to a total feedback of only  $0.5 \text{ W m}^{-2}$ . One way to look at these feedbacks is that the climate system is quite stable, with clouds and meridional transports limiting the impact of albedo changes. This may explain why some numerical models have difficulties creating the observed cooling

associated with the orbital forcing (e.g., Jackson and Broccoli 2003).

Ultimately, of course, a successful simulation of the inception does not necessarily need cooling, but an increased snow and ice cover to build ice sheets. In principle the increased snow accumulation seen in Fig. 1c could be due to increased snowfall or reduced snowmelt. The global moisture budgets reveal that outside the tropics OP115 has a larger poleward moisture transport than CONT, but this is largely confined to the midlatitudes and does not reach past the Arctic Circle (Fig. 4b). Thus, in contrast to the results of Vettoretti and Peltier (2003) the increase in snowfall is negligible compared to the reduction in snowmelt (not shown). The global net difference in melting and snowfall between OP115 and CONT leads to an implied snow accumulation that is equivalent to a sea level drop of 20 m in 10 000 years, some of it being due to the Baffin Island cold bias. This is less than the 50-m estimate based on sea level reconstructions between present day and 115 kya (e.g., Waelbroeck et al. 2002; Rohling et al. 2009; Siddall et al. 2010), but nonetheless it suggests that the model response is of the right magnitude.

#### 4. The role of the AMOC and the Labrador Sea gyre

The meridional heat transport of the AMOC is a major source of heat for the northern North Atlantic Ocean (e.g., Ganachaud and Wunsch 2000), but it is also believed to be susceptible to small perturbations (e.g., Marotzke 1990). This raises the possibility that the AMOC amplifies the orbital forcing, or even that this amplification is necessary for the Northern Hemisphere glaciations and terminations (e.g., Broecker 1998). In fact, JPML demonstrates that at least in one GCM changes in orbital forcing can lead to a weakening of the MOC and a subsequent large Northern Hemisphere cooling. Here, we revisit the connection between orbital forcing and AMOC strength with the CCSM4, which features improved physics and higher spatial resolution compared to JPML.

It turns out that for CCSM4, the OP115 scenario does not lead to a reduced AMOC, in contrast to the JPML results that show a 30% reduction of the AMOC strength under OP115 forcing. After branching off at year 500 of CONT, the AMOC in OP115 immediately weakens, and continues to do so until it reaches a minimum after approximately 60 years (Fig. 5a). It starts to recover around year 600, and reaches a mean value of  $15.3 \pm 0.7 \text{ Sv}$  ( $1 \text{ Sv} \equiv 10^6 \text{ m}^3 \text{ s}^{-1}$ ; years 751–800,  $0.7 \text{ Sv}$  is the standard deviation of the annual mean) at  $50^\circ\text{N}$ , slightly stronger than the  $14.8 \pm 0.7 \text{ Sv}$  in CONT. This is

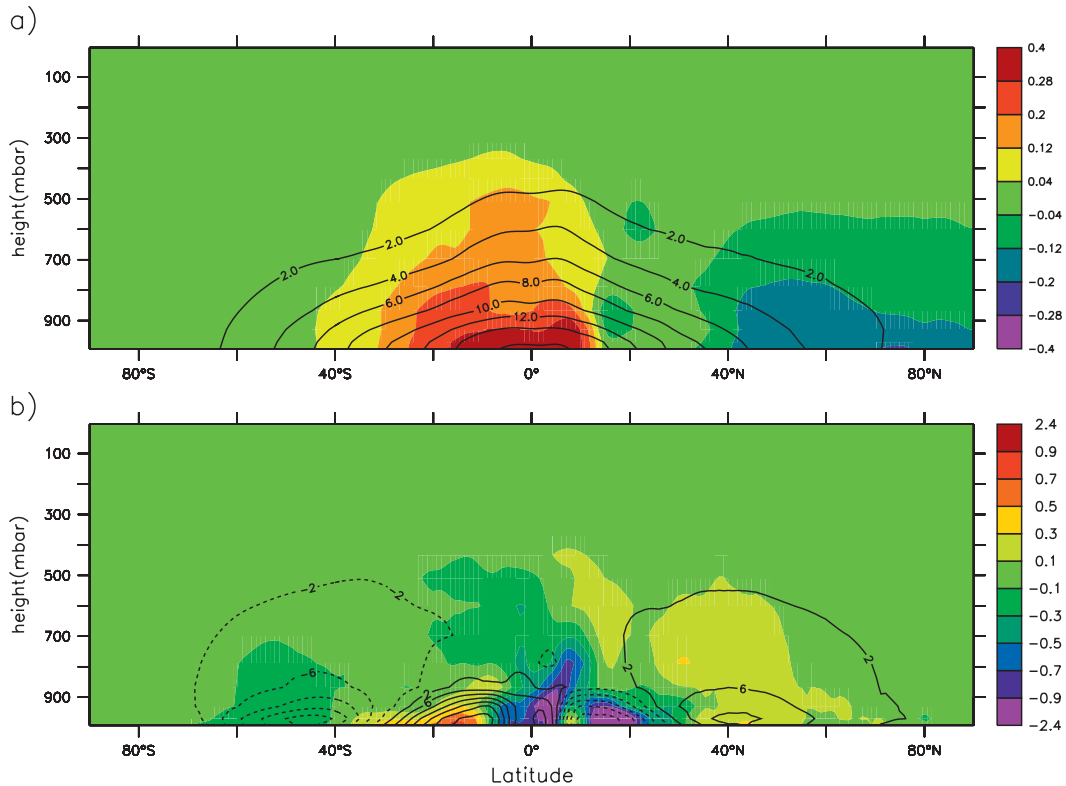


FIG. 4. (a) Difference in zonally averaged specific humidity between OP115 and CONT (color,  $\text{g kg}^{-1}$ ) and the zonally averaged specific humidity in CONT (contour interval  $2 \text{ g kg}^{-1}$ ). (b) Difference in zonally averaged meridional moisture transport between OP115 and CONT (color,  $\text{g kg}^{-1} \times \text{m s}^{-1}$ ) and the zonally averaged meridional moisture transport in CONT (contour interval  $2 \text{ g kg}^{-1} \times \text{m s}^{-1}$ ).

associated with an increase of heat transport from  $0.71 \pm 0.04$  PW to  $0.74 \pm 0.04$  PW (Fig. 5b). The depth of the AMOC in OP115 (as defined by the depth of the 0-Sv isoline at  $25^\circ\text{N}$ ) increases from the  $3870 \pm 390$  in CONT to 4800-m depth around year 600, and then rises again to  $3700 \pm 330$  m (not shown). The strength of the subpolar gyre, too, mirrors this decline and subsequent recovery with a mean strength of  $55.8 \pm 2.1$  Sv in CONT and  $55.0 \pm 1.8$  Sv in OP115 (Fig. 5c). Based on standard normal distributions, sample sizes of 50 annual means, and lag-1 autocorrelations between 0.3 and 0.6 the signs of the differences above are significant at a 99% level. By the end of this 300-yr development, the surface of the Irminger Sea and most of the subsurface subpolar Atlantic is warmer and saltier than in CONT, and the surface of the Labrador Sea is colder and fresher (Fig. 5d).

Much of this reorganization of the subpolar Atlantic can be explained by the analysis of sea ice extent and maximum ocean boundary layer depth, the latter being by construction the depth of a year's deepest convective event (Large et al. 1994). In CONT, convective activity can be seen all along the edge of the sea ice and south of Iceland (Fig. 6a). In OP115 the different orbital forcing

leads initially to more extensive sea ice in the Labrador Sea (Fig. 6b), because of the reduced summer insolation. The Irminger Sea, however, is under the influence of the warm North Atlantic Drift, which leads to only minor changes in the sea ice. The initial increase in sea ice concentration insulates the Labrador Sea from atmospheric forcing, and therefore inhibits convective activity and reduces the strength of the subpolar gyre (Fig. 5c). South of Iceland, without the effects of sea ice, the orbital forcing initially leads merely to a cooling of the surface water, and therefore a destabilization of the water column (Fig. 6c) and deeper convection (Fig. 6b). The intermediate depth warming seen in Figs. 6c and 5d is the direct result of the weaker Labrador Sea gyre: the weaker gyre leads to a poleward migration of the Gulf Stream and the North Atlantic Drift (Fig. 6d), with its associated influx of more spicy (warmer and saltier) water. For water of equal density, the atmosphere removes buoyancy more efficiently from spicier water (Jochum 2009), so that after 300 years the convective activity in the subpolar gyre is quite similar between CONT and OP115 (not shown), albeit in a different background state (Fig. 5d). Thus, the connection between subpolar gyre strength

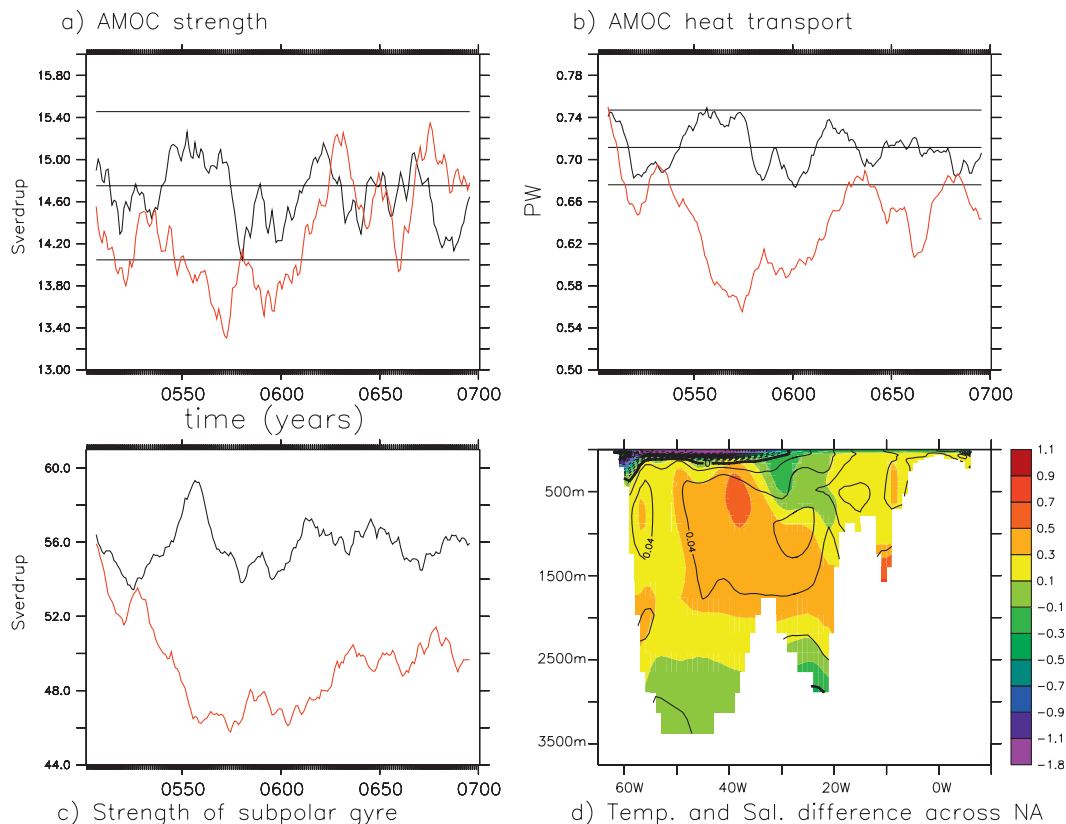


FIG. 5. (a) Strength of the annual mean AMOC (Sv) at  $50^{\circ}\text{N}$  for CONT (black) and OP115 (red). The straight black lines denote the mean and mean  $\pm 1$  standard deviation of the annual mean of CONT. Here, and in the (b) and (c), only years 501–700 are shown, because CONT ends at year 700; OP115 slowly approaches the values cited in the text. (b) As in (a), but for the meridional heat transport (PW). (c) Maximum strength of the subpolar gyre (Sv, typically the maximum is located between Greenland and Labrador). Again, the black line is based on CONT, the red on OP115. Note that all the time series have been smoothed with an 11-yr running mean. (d) Mean temperature (color) and salinity (contour interval: 0.02 psu, minimum:  $-0.4$  psu, maximum: 0.1 psu) difference between Labrador and Norway.

and subtropical spiciness advection acts as a negative feedback that stabilizes the gyre.

Another source of North Atlantic Deep Water is convection in the Norwegian Sea, which enters the subpolar gyre through the Denmark Strait and Faroe Bank Channel overflows. In CONT, this is a 5.2-Sv ( $\pm 0.4$  Sv) contribution to the AMOC. This value is determined by a parameterization and depends largely on the density differences between the water masses on either side of the ridges (Danabasoglu et al. 2010). North of the ridges, the changes in salinity and temperature largely compensate for each other so that the maximum boundary depth and density changes are minor (not shown). Thus, the transient response is determined by the behavior of the subpolar gyre, which leads to an initial cooling of the waters on the Atlantic side of the ridge, and then a recovery as the gyre and the AMOC strengthen (Fig. 6c). The cooling leads to minimum overflow of 4.1 Sv after

120 years (about 40 years after the minimum in AMOC and gyre strength) and then recovers toward a transport of 5.4 Sv in years 751–800 (not shown). Thus, the variability of the overflow strength, too, is controlled by the subpolar gyre.

In principle, the two mechanisms described above should have come into play in JPML as well. There, however, an increased freshwater export out of the Arctic led to a halocline catastrophe [see Bryan (1986) for a general discussion of this process]. It turns out that in CCSM4 with its finer spatial resolution there is a crucial third process that allows the AMOC to recover, which is not present in JPML: the freshwater flux through the Baffin Bay (Fig. 7). An analysis of the subpolar freshwater budget shows that its largest anomalies are the liquid freshwater transport through the Nares Strait and Northwest Passage (via the Baffin Bay), and the sea ice import from the Arctic into the subpolar

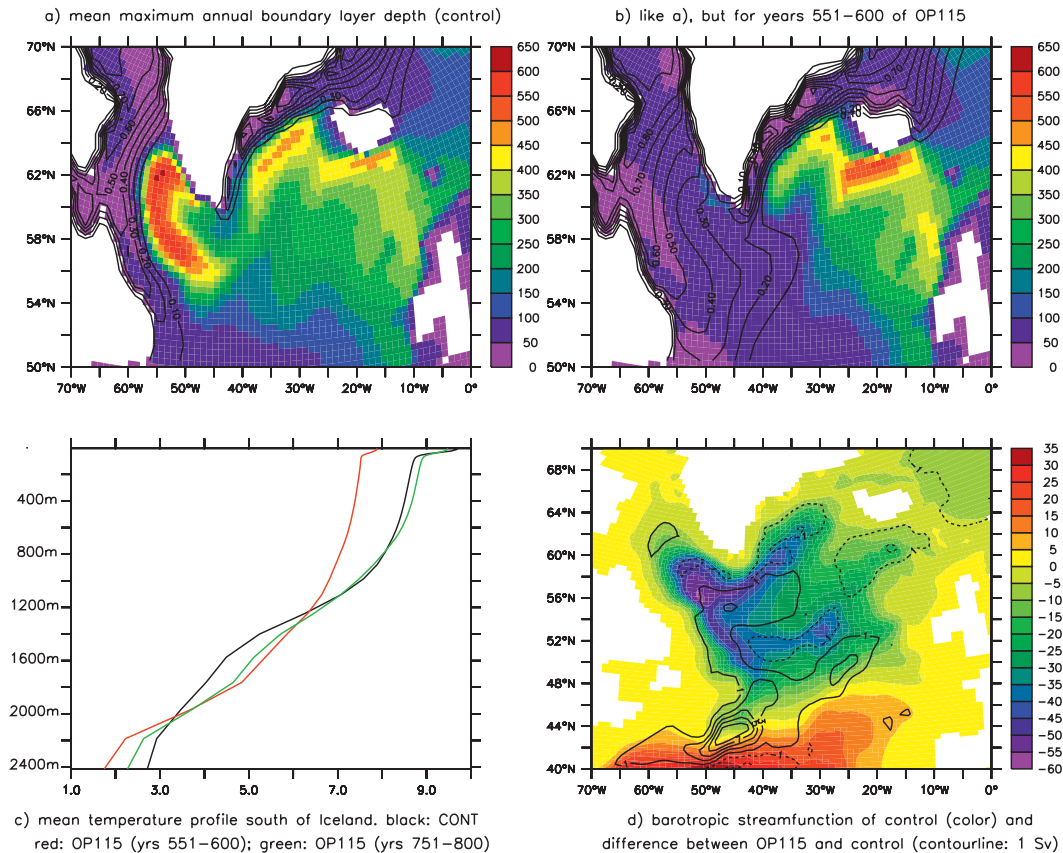


FIG. 6. (a) Mean maximum annual boundary layer depth (m, color) and annual mean sea ice concentration (contour lines: 10%) for CONT. (b) As in (a), but for years 551–600 of OP115. (c) Mean temperature profile south of Iceland. (d) Depth-integrated transport in CONT (color), and difference between OP115 and CONT (OP115–CONT, contour interval: 1 Sv).

Atlantic through the Fram Strait (Fig. 8). Immediately after changing the orbital forcing, the import of sea ice through the Fram Strait increases, and continues to increase for another 100 years. This is also happening in the coarse-resolution version and leads to the halocline catastrophe (JPML). In the present experiment, however, a good part of the increased ice import is compensated by reduced inflow of liquid freshwater into the Baffin Bay. The strength of the flow into Baffin Bay is determined by the sea surface height difference between the Arctic and the Labrador Sea (Prinsenbergh and Bennett 1987; Kliem and Greenberg 2003; Jahn et al. 2010). This difference is reduced from 70 cm in CONT to 50 cm during the years 551–600 in OP115 (not shown).

Thus, there are two negative feedbacks by which the effect of orbital forcing on the AMOC is minimized. Both work through the subpolar gyre. First, increased sea ice cover reduces its strength; this brings in spicier subtropical water, which is more susceptible to convection. Second, the reduced gyre strength leads to a reduced pressure difference between the Arctic and the Labrador

Sea, thereby reducing the import of freshwater through the Nares Strait and Northwest Passage. The correlation between a weaker subpolar gyre and an increased influx of subtropical salty water has actually been observed over the last 20 years (Hátun et al. 2005; Hakkinen and Rhines 2009), albeit without attributing an ultimate cause for these changes. The inception study by Born et al. (2010), also finds that an increased sea ice export through the Denmark Strait at 115 kya leads to a weakening of the subpolar gyre, increased influx of subtropical water, and subsequent stabilization of the subpolar gyre. The spatial resolution of their study OGCM is finer than the one of JPML, but coarser than the present resolution, and their study did not attribute any importance to the freshwater transport through Baffin Bay.

To what extent the present feedbacks are relevant in the real world will depend on an accurate representation of the Arctic and subpolar physics. A detailed discussion of model performance and biases is provided in Danabasoglu et al. (2012); here we will limit ourselves to a quantification of some of the key processes. As in

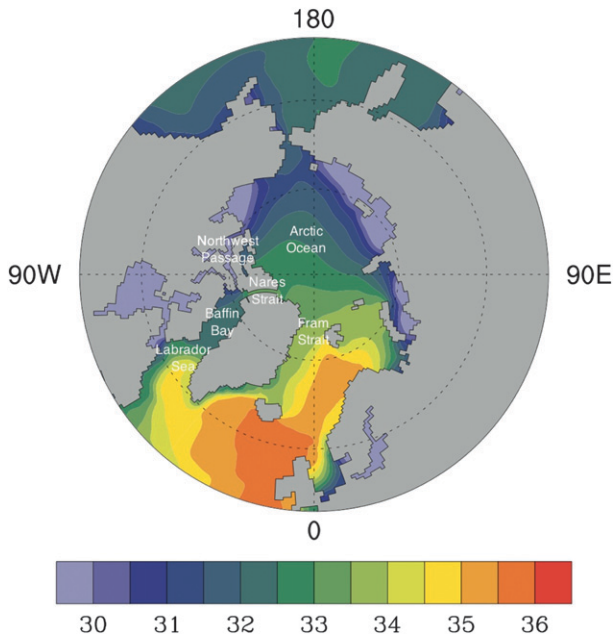


FIG. 7. Sea surface salinity (psu) in CONT north of 50°N. Also shown are the locations of several seas and passages that are mentioned in the text.

the observations (Dickson and Brown 1994; Vage et al. 2009), deep-water formation occurs in the Irminger, Labrador, and the Greenland Seas with maximum boundary layer depths of approximately 1000 m in the latter two, and 800 m in the former. However, deep convection is not observed south of Iceland and this is

a major bias in the model. The product of the Denmark Strait and Faroe Bank Channel overflow water is well reproduced with 5.2 Sv when compared to the recent observational estimates of 6.5 Sv (Girton and Sanford 2003; Mauritzen et al. 2005). The shutdown of the Labrador Sea convection in OP115 leads to 1-Sv reduction in the AMOC, which is consistent with recent evidence that the contribution of Labrador Sea convection to the AMOC is less than 2 Sv (Pickart and Spall 2007). With 19.5 Sv, the strength of the AMOC at 26.5°N is close to the observed value of 18.7 Sv (Kanzow et al. 2009). The freshwater budget and the sea ice properties of the Arctic Ocean are also well represented in CCSM4 (Jahn et al. 2012), the main bias being that the March sea ice edge extends too far toward Iceland. This general assessment of the model performance is encouraging, but it should be kept in mind that the response of the AMOC to disturbances can be critically dependent on poorly constrained mixing processes (e.g., Schmittner and Weaver 2001; Saenko et al. 2003) or the still not yet understood forcing by the Southern Ocean (e.g., Toggweiler and Samuels 1995; Radko and Kamenkovich 2011).

The present authors are aware of only one proxy tracer-based analysis of the AMOC strength that stretches past 115 kya, and it suggests that the AMOC started weakening only several thousand years after the beginning of the last glacial inception (Guihou et al. 2010). Other estimates of past AMOC strength are based mostly on proxies from deep ocean cores for the Last Glacial Maximum (LGM; 21 kya). It is not clear if anything can be learned about the AMOC 115 kya by studying the

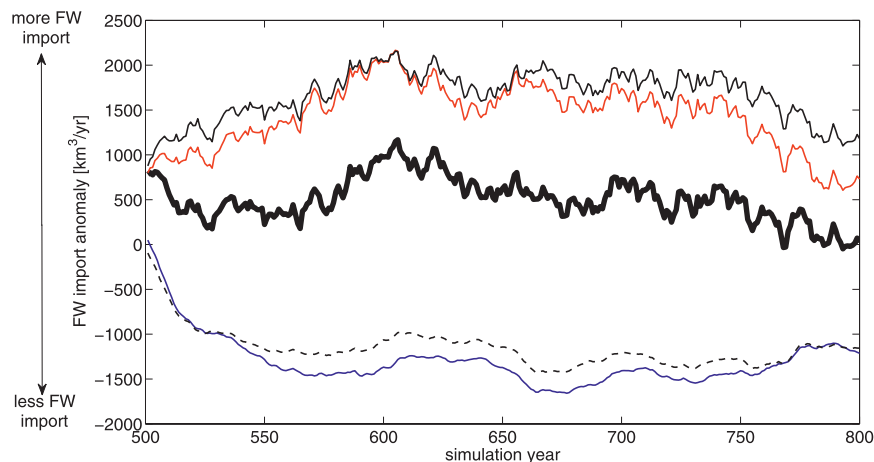


FIG. 8. Change in the total freshwater (FW) import from the Arctic Ocean to the subpolar Atlantic (thick black line) in OP115 compared to the mean of years 501–700 from CONT. This anomaly is also shown split up into the contribution of the FW import east (red line) and west (blue line) of Greenland, as well as split up into the solid FW import (mainly east of Greenland; solid thin black line) and the liquid FW import (dashed line). The fluxes are computed relative to a salinity of 34.8 (Aagaard and Carmack 1989).

LGM. One could argue, however, that somewhere between the interglacial AMOC state and the glacial maximum AMOC state the AMOC would be in a 115 kya state. This assumes a simplified view of the ocean circulation, but it would allow us to provide upper and lower bounds for the 115-kya AMOC strength—if we knew the AMOC strength during the LGM. The most widely used proxies to infer ocean circulation patterns during the LGM are carbon isotopes ( $\delta^{13}\text{C}$ ; e.g., Duplessy et al. 1988), cadmium–calcium (Cd/Ca; e.g., Marchitto and Broecker 2006) and protactinium–thorium ratios in benthic foraminifera (Pa/Th; e.g., McManus et al. 2004), magnetic grain sizes (Kissel et al. 1999; Stanford et al. 2006), and estimates of the density gradient across the Atlantic basin based on oxygen isotope profiles ( $\delta^{18}\text{O}$ ; Lynch-Stieglitz et al. 1999). Measurements of sortable silts have been used to infer rates of past deep-ocean flows (McCave et al. 1995). For each of these tracers there are studies that indicate a weaker or shallower AMOC during the LGM (e.g.; 2007; Gherardi et al. 2009; Lynch-Stieglitz et al. 2006, 2007; McCave et al. 1995), but the more recent application of rigorous statistical tools suggests that the available database is currently not sufficient to reject the hypothesis of an unchanged AMOC during the LGM (e.g., Gebbie and Huybers 2006; Marchal and Curry 2008; Peacock 2010). Interestingly it is not only the data that is inconclusive; LGM simulations, too, do not agree on the sign of the difference between the present-day and LGM AMOC (Otto-Bliesner et al. 2007). Thus, the present model result of 115-kya orbital forcing having no impact on the strength of the AMOC is consistent with the available observations.

## 5. Summary and discussion

It is shown here that the same CCSM4 version that realistically reproduces the present-day climate, also shows, when subjected to orbital forcing from 115 kya, increased areas of perennial snow in the areas where glacial reconstructions put the origin of the glacial ice sheets. Furthermore, the difference in snow deposition between OP115 and CONT is of the same order of magnitude as the reconstructions based on sea level data. CCSM4 achieves this by the most basic mechanism, which was already postulated by Milankovitch (1941): reduced Northern Hemisphere summer insolation reduces snow and sea ice melt, which leads to larger areas with perennial snow and sea ice, and increased albedo. This, in turn, further reduces melting, leading to the positive snow/ice–albedo feedback.

This positive feedback is opposed and almost compensated for by increased meridional heat transport in

the atmosphere, and by reduced low cloud cover over the Arctic. The former is on solid theoretical grounds (e.g., Stone 1978) and has support from other GCM studies (e.g., Shaffrey and Sutton 2006), but the physics of low Arctic clouds is one of the weak points of current GCMs (e.g., Kay et al. 2011). This does not mean that the CCSM4 response of Arctic clouds to insolation is necessarily wrong. The paucity of observations relevant for sea ice–cloud feedbacks means, however, that there have been only a few opportunities to test this aspect of the model.

An equally large source of uncertainty is the stability of the AMOC. However, the fact that CCSM4 is able to recreate a reasonable inception scenario without an active ocean removes the 115-kya scenario as a test bed for the ocean model. As discussed in section 3, the observations are not conclusive either, nor is there a comprehensive theory for the AMOC strength [see Kuhlbrodt et al. (2007) for a recent review]. Thus, from the present set of experiments we can only conclude that ocean feedbacks are not necessary for glacial inception, but we cannot rule out that the ocean did play a role.

Although due in part to the Baffin Island cold bias, the OP115 experiment's increase in perennial snow cover and snow deposition is encouraging. Of course, the present study can only be a first step toward reproducing the glacial inception in a GCM. It still remains to be shown that the OP115 climate allows for the growth of the Scandinavian, Siberian, and Laurentide ice sheets. More importantly, though, the lack of any significant Southern Hemisphere polar response needs explaining (Fig. 1). While Petit et al. (1999) suggests that Antarctica cooled by about  $10^{\circ}\text{C}$  during the last inception, the more recent high-resolution analysis by Jouzel et al. (2007) suggest that it was only slightly cooler than today (less than  $3^{\circ}\text{C}$  at the European Project for Ice Coring in Antarctica (EPICA) Dome C site on the Antarctic Plateau). Of course, there are substantial uncertainties in reconstructing Antarctic temperatures (e.g., Stenni et al. 2010), but there are also significant biases in the Southern Ocean wind stress and sea ice representation in CCSM (Landrum et al. 2012). The sea ice bias is the result of overly strong Southern Ocean winds (Holland and Raphael 2006)—a problem that, strangely enough, has been unresolved since Boville (1991).

Thus, while the present study finally provides numerical support for the Milankovitch hypothesis of glacial inception, it also identifies three foci of future research: first, the sensitivity of Arctic clouds to climate fluctuation needs to be validated and possibly improved upon; second, the Southern Ocean sea ice concentration and the strength of the zonal winds in CCSM need to become more realistic; and third the temperature biases

of the northern high-latitude continents have to be reduced.

*Acknowledgments.* The authors are supported by NSF through NCAR. The participation of DAB is made possible through funding under NSF-OPP Grant 0908675, and participation of JTF is made possible through funding under NASA Contract NNG06GB91G. The computations were made possible by the Computational Information Systems Laboratory at NCAR. The suggestions of three anonymous reviewers led to significant improvements to the manuscript. The authors thank Dave Lawrence and Keith Oleson for explaining the intricacies of the snow budget, and trout fishing in America for inspiration.

#### REFERENCES

- Aagaard, K., and E. C. Carmack, 1989: The role of sea ice and other fresh water in the Arctic circulation. *J. Geophys. Res.*, **94**, 14 485–14 498.
- Andrews, J. T., and M. A. W. Mahaffy, 1976: Growth-rate of Laurentide ice sheet and sea-level lowering (with emphasis on 115,000 BP sea-level low). *Quat. Res.*, **6**, 167–183.
- Berger, A., and M. F. Loutre, 1991: Insolation values for the climate of the last 10,000,000 years. *Quat. Sci. Rev.*, **10**, 297–317.
- Born, A., K. H. Nisancioglu, and P. Braconnot, 2010: Sea ice induced changes in the ocean circulation during the Eemian. *Climate Dyn.*, **35**, 1361–1371.
- Boville, B. A., 1991: Sensitivity of simulated climate to model resolution. *J. Climate*, **4**, 469–485.
- Broecker, W. S., 1998: Paleocan circulation during the last deglaciation: A bipolar seesaw? *Paleoceanography*, **13**, 119–121.
- Bryan, F. O., 1986: High-latitude salinity effects and interhemispheric thermohaline circulations. *Nature*, **323**, 301–304.
- Calov, R., A. Ganopolski, M. Claussen, V. Petoukhov, and R. Greve, 2005: Transient simulation of the last glacial inception. Part I: Glacial inception as a bifurcation in the climate system. *Climate Dyn.*, **24**, 545–561.
- Capron, E., and Coauthors, 2010: Synchronising EDML and North-GRIP ice cores using delta O-18 of atmospheric oxygen (delta O-18(atm)) and CH4 measurements over MIS5 (80-123 kyr). *Quat. Sci. Rev.*, **29**, 222–234.
- Collins, W. D., and Coauthors, 2006: The Community Climate System Model version 3 (CCSM3). *J. Climate*, **19**, 2122–2143.
- Crucifix, M., and M. F. Loutre, 2001: Transient simulations over the last interglacial period (126-115kyrBP): Feedback and forcing analysis. *Climate Dyn.*, **19**, 417–433.
- Danabasoglu, G., and P. Gent, 2009: Equilibrium climate sensitivity: Is it accurate to use a slab ocean model? *J. Climate*, **22**, 2494–2499.
- , W. G. Large, and B. P. Briegleb, 2010: Climate impacts of parameterized Nordic Sea overflows. *J. Geophys. Res.*, **115**, C11005, doi:10.1029/2010JC006243.
- , and Coauthors, 2012: The CCSM4 ocean component. *J. Climate*, **25**, 1361–1389.
- Dickson, R. R., and J. Brown, 1994: The production of North Atlantic Deep Water: Sources, rates, and pathways. *J. Geophys. Res.*, **99**, 12 319–12 341.
- Dong, B., and P. J. Valdes, 1995: Sensitivity studies of Northern Hemisphere glaciation using an atmospheric general circulation model. *J. Climate*, **8**, 2471–2473.
- Duplessy, J. C., N. J. Shackleton, R. G. Fairbanks, L. Labeyrie, D. Oppo, and N. Kalle, 1988: Deepwater source variations during the last climatic cycle and their impact on the global deepwater circulation. *Paleoceanography*, **3**, 343–360.
- Edwards, M. H., 1986: Digital image processing and interpretation of local and global bathymetric data. M.S. thesis, Department of Engineering, Washington University, 212 pp.
- Gallimore, R. G., and J. E. Kutzbach, 1996: Role of orbitally induced changes in tundra area in the onset of glaciation. *Nature*, **381**, 503–505.
- Ganachaud, A., and C. Wunsch, 2000: Improved estimates of global ocean circulation, heat transport and mixing from hydrographic data. *Nature*, **408**, 453–457.
- Ganopolski, A., R. Calov, and M. Claussen, 2010: Simulation of the last glacial cycle with a coupled climate ice-sheet model of intermediate complexity. *Climate Past*, **6**, 229–244.
- Gebbie, J., and P. Huybers, 2006: Meridional circulation during the Last Glacial Maximum explored through a combination of South Atlantic d18O observations and a geostrophic inverse model. *Geochem. Geophys. Geosyst.*, **7**, 394–407.
- Gent, P. R., and Coauthors, 2011: The Community Climate System Model version 4. *J. Climate*, **24**, 4973–4991.
- Gherardi, J.-M., L. Labeyrie, S. Nave, R. Francois, J. F. McManus, and E. Cortijo, 2009: Glacial-interglacial circulation changes inferred from <sup>231</sup>Pa/<sup>230</sup>Th sedimentary record in the North Atlantic region. *Paleoceanography*, **24**, PA2204, doi:10.1029/2008PA001696.
- Girton, J. B., and T. B. Sanford, 2003: Descent and modification of the overflow plume in the Denmark Strait. *J. Phys. Oceanogr.*, **33**, 1351–1363.
- Groeger, M., E. Maier-Reimer, U. Mikolajewicz, G. Schurgers, M. Vizcaino, and A. Winguth, 2007: Changes in the hydrological cycle, ocean circulation, and carbon/nutrient cycling during the last interglacial and glacial transition. *Paleoceanography*, **22**, PA4205, doi:10.1029/2006PA001375.
- Gualtieri, L., S. Vartanyan, J. Brigham-Grette, and P. M. Anderson, 2003: Pleistocene raised marine deposits on Wrangle Island, northeast Siberia and implications for the presence of an East Siberian ice sheet. *Quat. Res.*, **59**, 399–410.
- Guihou, A., S. Pichat, S. Nave, A. Govin, L. Labeyrie, E. Michel, and C. Waelbroeck, 2010: Late slowdown of the Atlantic Meridional Overturning Circulation during the Last Glacial Inception: New constraints from sedimentary (<sup>231</sup>Pa/<sup>230</sup>Th). *Earth Planet. Sci. Lett.*, **289**, 520–529.
- Hakkinen, S., and P. B. Rhines, 2009: Shifting surface currents in the northern North Atlantic Ocean. *J. Geophys. Res.*, **114**, C04005, doi:10.1029/2008JC004883.
- Hall, A., A. Clement, D. W. J. Thompson, A. Broccoli, and C. Jackson, 2005: The importance of atmospheric dynamics in the Northern Hemisphere wintertime climate response to changes in the earth's orbit. *J. Climate*, **18**, 1315–1325.
- Hátun, H., A. B. Sando, H. Drange, B. Hansen, and H. Valdimarsson, 2005: Influence of the Atlantic subpolar gyre on the thermohaline circulation. *Science*, **309**, 1841–1844.
- Hays, J. D., J. Imbrie, and N. J. Shackleton, 1976: Variations in the Earth's orbit, pacemaker of the ice ages. *Science*, **194**, 1121–1132.
- Holland, M. M., and M. N. Raphael, 2006: Twentieth century simulation of the southern hemisphere climate in coupled models. Part II: Sea ice conditions and variability. *Climate Dyn.*, **26**, 229–245.

- Huybers, P., and C. Wunsch, 2004: A depth-derived Pleistocene age model: Uncertainty estimates, sedimentation variability, and nonlinear climate change. *Paleoceanography*, **19**, PA1028, doi:10.1029/2002PA000857.
- Imbrie, J., and Coauthors, 1992: On the structure and origin of major glacial cycles. 1. Linear responses to Milankovitch forcing. *Paleoceanography*, **7**, 701–738.
- Jackson, C. S., and A. J. Broccoli, 2003: Orbital forcing of Arctic climate: Mechanisms of climate response and implications for continental glaciation. *Climate Dyn.*, **21**, 539–557.
- Jahn, A., L. B. Tremblay, R. Newton, M. M. Holland, L. A. Mysak, and I. A. Dmitrenko, 2010: A tracer study of the Arctic Ocean's liquid freshwater export variability. *J. Geophys. Res.*, **115**, C07015, doi:10.1029/2009JC005873.
- , and Coauthors, 2012: Late-twentieth-century simulation of Arctic sea-ice and ocean properties in the CCSM4. *J. Climate*, **25**, 1431–1452.
- Jochum, M., 2009: Impact of latitudinal variations in vertical diffusivity on climate simulations. *J. Geophys. Res.*, **114**, C01010, doi:10.1029/2008JC005030.
- , S. Peacock, J. K. Moore, and K. Lindsay, 2010: Response of carbon fluxes and climate to orbital forcing changes in the Community Climate System Model. *Paleoceanography*, **25**, PA3201, doi:10.1029/2009PA001856.
- Jouzel, J., and Coauthors, 2007: Orbital and millennial Antarctic climate variability over the past 800,000 years. *Science*, **317**, 793–796.
- Kageyama, M., S. Charbit, C. Ritz, M. Khodri, and G. Ramstein, 2004: Quantifying ice-sheet feedbacks during the last glacial inception. *Geophys. Res. Lett.*, **31**, L24203, doi:10.1029/2004GL021339.
- Kanzow, T., H. L. Johnson, D. P. Marshall, S. A. Cunningham, J. J.-M. Hirschi, A. Mujahid, H. L. Bryden, and W. E. Johns, 2009: Basinwide integrated volume transports in an eddy-filled ocean. *J. Phys. Oceanogr.*, **39**, 3091–3110.
- Kaspar, F., and U. Cubasch, 2007: Simulation of the Eemian interglacial and possible mechanisms for the glacial inception. Geological Society of America, Special Paper 426, 14 pp.
- Kay, J. E., and A. Gettelman, 2009: Cloud influence on and response to seasonal Arctic sea ice loss. *J. Geophys. Res.*, **114**, D18204, doi:10.1029/2009JD011773.
- , K. Raeder, A. Gettelman, and J. Anderson, 2011: The boundary layer response to recent Arctic sea ice loss and implications for high-latitude climate feedbacks. *J. Climate*, **24**, 428–447.
- Khodri, M., Y. Leclainche, G. Ramstein, P. Braconnot, O. Marti, and E. Cortijo, 2001: Simulating the amplification of orbital forcing by ocean feedbacks in the last glaciation. *Nature*, **410**, 570–574.
- , G. Ramstein, D. Paillard, J. C. Duplessy, M. Kageyama, and A. Ganopolski, 2003: Modelling the climate evolution from the last interglacial to the start of the last glaciation: The role of Arctic Ocean freshwater budget. *Geophys. Res. Lett.*, **30**, 1606, doi:10.1029/2003GL017108.
- Kissel, C., C. Laj, L. Labeyrie, T. Dokken, A. Voelker, and D. Blamart, 1999: Rapid climate variations during marine isotope stage 3: Magnetic analysis of sediments from Nordic Seas and North Atlantic. *Earth Planet. Sci. Lett.*, **171**, 489–502.
- Kleman, J., K. Jansson, H. De Angelis, A. P. Stroeven, C. Hättestrand, G. Alm, and N. Glasser, 2010: North American Ice Sheet build-up during the last glacial cycle, 115–21 kyr. *Quat. Sci. Rev.*, **29**, 2036–2051.
- Kliem, N., and D. A. Greenberg, 2003: Diagnostic simulations of the summer circulation in the Canadian Arctic Archipelago. *Atmos.–Ocean*, **41**, 273–289.
- Kuhlbrodt, T., A. Griesel, M. Montoya, A. Levermann, M. Hofmann, and S. Rahmstorf, 2007: On the driving processes of the Atlantic meridional overturning circulation. *Rev. Geophys.*, **45**, RG2001, doi:10.1029/2004RG000166.
- Landrum, L., M. M. Holland, D. Schneider, and E. Hunke, 2012: Antarctic sea ice climatology, variability, and late-twentieth-century change in CCSM4. *J. Climate*, in press.
- Large, W. G., J. C. McWilliams, and S. C. Doney, 1994: Oceanic vertical mixing—A review and a model with nonlocal parameterization. *Rev. Geophys.*, **32**, 363–403.
- Lawrence, D. M., and Coauthors, 2010: Parameterization improvements and functional and structural advances in version 4 of the Community Land Model. *J. Adv. Model. Earth Syst.*, **3**, M03001, doi:10.1029/2011MS000045.
- Lynch-Stieglitz, J., W. B. Curry, and N. Slowey, 1999: Weaker Gulf Stream in the Florida Straits during the Last Glacial Maximum. *Nature*, **402**, 644–648.
- , —, D. W. Oppo, U. S. Ninneman, C. D. Charles, and J. Munson, 2006: Meridional overturning circulation in the South Atlantic at the last glacial maximum. *Geochem. Geophys. Geosyst.*, **7**, 1–14.
- , and Coauthors, 2007: Atlantic meridional overturning circulation during the Last Glacial Maximum. *Science*, **316**, 66–69.
- Marchal, O., and W. B. Curry, 2008: On the abyssal circulation in the glacial Atlantic. *J. Phys. Oceanogr.*, **38**, 2014–2037.
- Marchitto, T. M., and W. S. Broecker, 2006: Deep water mass geometry of the glacial Ocean: A review of constraints from the paleonutrient proxy Cd/Ca. *Geochem. Geophys. Geosyst.*, **7**, Q12003, doi:10.1029/2006GC001323.
- Marotzke, J., 1990: Instabilities and multiple equilibria of the thermohaline circulation. Ph.D. thesis, Berichte vom Institut fuer Meereskunde Kiel 194, 126 pp.
- Mauritzen, C., J. Price, T. Sanford, and D. Torres, 2005: Circulation and mixing in the Faroer Channels. *Deep-Sea Res. I*, **52**, 883–913.
- McCave, I., B. Manighetti, and N. Beveridge, 1995: Circulation in the glacial North Atlantic inferred from grain size measurements. *Nature*, **374**, 149–152.
- McManus, J. F., R. Francois, J.-M. Gherardi, L. D. Keigwin, and S. Brown-Leger, 2004: Collapse and rapid resumption of the AMOC linked to deglacial climate changes. *Nature*, **428**, 834–837.
- Milankovitch, M., 1941: *Canon of Insolation and the Ice-Age Problem*. Israel Program for Scientific Translations, 484 pp.
- Neale, R., J. Richter, and M. Jochum, 2008: The impact of convection on ENSO: From a delayed oscillator to a series of events. *J. Climate*, **21**, 5904–5924.
- Oleson, K. W., and Coauthors, 2010: Technical description of version 4.0 of the Community Land Model. NCAR Tech. Note TN-478+STR, 257 pp.
- Otieno, F. O., and D. H. Bromwich, 2009: Contribution of atmospheric circulation to inception of the Laurentide ice sheet at 116 kyr BP. *J. Climate*, **22**, 39–57.
- Otto-Bliesner, B. L., C. D. Hewitt, T. M. Marchitto, E. Brady, A. Abe-Ouchi, M. Crucifix, S. Murakami, and S. L. Weber, 2007: Last Glacial Maximum ocean thermohaline circulation: PMIP2 model intercomparisons and data constraints. *Geophys. Res. Lett.*, **34**, L12706, doi:10.1029/2007GL029475.
- Peacock, S., 2010: Comment on “Glacial-interglacial circulation changes inferred from  $^{231}\text{Pa}/^{230}\text{Th}$  sedimentary record in the

- North Atlantic region" by J.-M. Gherardi et al. *Paleoceanography*, **25**, PA2206, doi:10.1029/2009PA001835.
- , 2012: Projected twenty-first-century changes in temperature, precipitation, and snow cover over North America in CCSM4. *J. Climate*, in press.
- Petit, J., and Coauthors, 1999: Climate and atmospheric history of the past 420,000 years from the Vostok ice core, Antarctica. *Nature*, **399**, 429–436.
- Pickart, R. S., and M. A. Spall, 2007: Impact of Labrador Sea convection on the North Atlantic meridional overturning circulation. *J. Phys. Oceanogr.*, **37**, 2207–2227.
- Prinsenberg, S. J., and E. B. Bennett, 1987: Mixing and transport in Barrow Strait, the central part of the Northwest Passage. *Cont. Shelf Res.*, **7**, 913–935.
- Radko, T., and I. Kamenkovich, 2011: Semi-adiabatic model of the deep stratification and meridional overturning. *J. Phys. Oceanogr.*, **41**, 757–779.
- Reeh, N., C. Mayer, H. Miller, H. H. Thomsen, and A. Weidick, 1999: Present and past climate control on fjord glaciations in Greenland: Implications for IRD-deposition in the sea. *Geophys. Res. Lett.*, **26**, 1039–1042.
- Rohling, E. J., K. Grant, M. Bolshaw, A. P. Roberts, M. Siddall, C. Hemleben, and M. Kucera, 2009: Antarctic temperature and global sea level closely coupled over the past five glacial cycles. *Nat. Geosci.*, **2**, 500–504, doi:10.1038/NGEO557.
- Saenko, O. A., E. C. Wiebe, and A. J. Weaver, 2003: North Atlantic response to the above-normal export of sea ice from the Arctic. *J. Geophys. Res.*, **108**, 3224, doi:10.1029/2001JC001166.
- Schmittner, A., and A. J. Weaver, 2001: Dependence of multiple climate states on ocean mixing parameters. *Geophys. Res. Lett.*, **28**, 1027–1030.
- Shaffrey, L., and R. Sutton, 2006: Bjerknes compensation and the decadal variability of the energy transports in a coupled climate model. *J. Climate*, **19**, 1167–1181.
- Siddall, M., M. R. Kaplan, J. M. Schaefer, A. Putnam, M. A. Kelly, and B. Goehring, 2010: Changing influence of Antarctic and Greenlandic temperature records on sea-level over the last glacial cycle. *Quat. Sci. Rev.*, **29**, 410–423.
- Stanford, J. D., E. J. Rohling, S. E. Hunter, A. P. Roberts, S. O. Rasmussen, E. Bard, J. McManus, and R. G. Fairbanks, 2006: Timing of meltwater pulse 1a and climate responses to meltwater injections. *Paleoceanography*, **21**, PA4103, doi:10.1029/2006PA001340.
- Stenni, B., and Coauthors, 2010: The deuterium excess records of EPICA Dome C and Dronning Maud Land ice cores. *Quat. Sci. Rev.*, **29**, 146–159.
- Stommel, H., 1961: Thermohaline convection with two stable regimes of flow. *Tellus*, **13**, 224–230.
- Stone, P. H., 1978: Constraints on dynamical transports of energy on a spherical planet. *Dyn. Atmos. Oceans*, **2**, 123–139.
- Svendsen, J. I., and Coauthors, 2004: Late Quaternary ice sheet history of northern Eurasia. *Quat. Sci. Rev.*, **23**, 1229–1271.
- Syktus, J., H. Gordon, and J. Chappell, 1994: Sensitivity of a coupled atmosphere-dynamic upper ocean GCM to variations of CO<sub>2</sub>, solar constant, and orbital forcing. *Geophys. Res. Lett.*, **21**, 1599–1602.
- Thompson, W. G., and S. L. Goldstein, 2005: Open-system coral ages reveal persistent suborbital sea-level changes. *Science*, **308**, 401–404.
- Timm, O., A. Timmermann, A. Abe-Ouchi, F. Saito, and T. Segawa, 2008: On the definition of seasons in paleoclimate simulations with orbital forcing. *Paleoceanography*, **23**, PA2221, doi:10.1029/2007PA001461.
- Toggweiler, J., and B. Samuels, 1995: Effect of the Drake Passage on the global thermohaline circulation. *Deep-Sea Res.*, **42**, 477–500.
- Tziperman, E., M. E. Raymo, P. Huybers, and C. Wunsch, 2006: Consequences of pacing the Pleistocene 100 kyr ice ages by nonlinear phase locking to Milankovitch forcing. *Paleoceanography*, **21**, PA4206, doi:10.1029/2005PA001241.
- Vage, K., and Coauthors, 2009: Surprising return of deep convection to the subpolar North Atlantic ocean in winter 2007–2008. *Nat. Geosci.*, **2**, 67–72, doi:10.1038/NGEO382.
- Vaughan, D. G., J. L. Bamber, M. Giovinetto, J. Russell, A. P. R. Cooper, 1999: Reassessment of net surface mass balance in Antarctica. *J. Climate*, **12**, 933–946.
- Vavrus, S., G. Phillipon-Berthier, J. E. Kutzbach, and W. F. Ruddiman, 2011: The role of GCM resolution in simulating glacial inception. *Holocene*, **16**, 1–12.
- Vettoretti, G., and W. R. Peltier, 2003: Post-Eemian glacial inception. Part II: Elements of a cryospheric moisture pump. *J. Climate*, **16**, 912–927.
- , and —, 2011: The impact of insolation, greenhouse gas forcing and ocean circulation changes on glacial inception. *Holocene*, **16**, 1–15.
- Waelbroeck, C., L. Labeyrie, E. Michel, J. C. Duplessy, J. F. McManus, K. Lambeck, E. Balbon, and M. Labracherie, 2002: Sea-level and deep water temperature changes derived from benthic foraminifera isotopic records. *Quat. Sci. Rev.*, **21**, 295–305.
- Wang, Z., and L. Mysak, 2002: Simulation of the last glacial inception and rapid ice sheet growth in the McGill Paleoclimate Model. *Geophys. Res. Lett.*, **29**, 2102, doi:10.1029/2002GL015120.